

## RESEARCH ARTICLE

# Development, Characterization and Optimization of N-acetylcysteine-loaded Solid Lipid Particles: *In-vitro* and *In-vivo* Study

Bhavana Madupoju<sup>1</sup>, Rapaka S. Raju<sup>2</sup>, Prasanna K. Desu<sup>2\*</sup>, GSN Koteswara Rao<sup>3</sup>, Rajasekhar R. Alavala<sup>4</sup>, Rama D. Amara<sup>5</sup>, G Chakravarthi<sup>2</sup>

<sup>1</sup>Department of Pharmaceutics, Nalanda College of Pharmacy, Cherlapally, Nalgonda, Telangana, India.

<sup>2</sup>Department of Pharmacy, Koneru Lakshmaiah Education Foundation, Vaddeswaram, Guntur, Andhra Pradesh, India.

<sup>3</sup>Department of Pharmacy, School of Medical and Allied Sciences, Galgotias University, Greater Noida, Uttar Pradesh, India

<sup>4</sup>Shobhaben Pratapbhai Patel School of Pharmacy and Technology Management, SVKM's NMIMS, , Mumbai, Maharashtra, India

<sup>5</sup>Department of English, Koneru Lakshmaiah Education Foundation, Vaddeswaram, Guntur, Andhra Pradesh India.

Received: 16<sup>th</sup> July, 2022; Revised: 26<sup>th</sup> August, 2022; Accepted: 05<sup>th</sup> September, 2022; Available Online: 25<sup>th</sup> September, 2022

## ABSTRACT

The purpose of the present investigation was to formulate N-acetyl cysteine (NAC) loaded solid lipid nanoparticles (SLNs), aiming to obtain an effective formulation to ensure a prolonged controlled release in liver & lung infections. In this research work, SLNs were prepared by hot homogenization method using Glyceryl monostearate, Soya lecithin, polysorbate 80, tween 40 and 80. Prepared SLNs were characterized for their physicochemical parameters. The optimized formulation yielded nanoparticles with an approximate diameter of  $159.10 \pm 15.36$ , a polydispersity index of 0.168, a zeta potential of  $-50.33$  mV and entrapment efficiency of  $86.32 \pm 1.24\%$ . An *in-vitro* dissolution analysis revealed the controlled release of contents from SLNs over 8 hours with 95.25% of the drug released. Differential scanning calorimetry thermograms showed drugs in drug-loaded nanoparticles and the absence of decomposition exotherms, suggesting improved physical drug stability in developed formulations. Negligible changes in drug peaks in Fourier transform infrared spectra revealed no interaction between nanoparticle components. A spherical morphology revealed spherical NAC-SLNs. X-ray diffraction (XRD) study indicated the crystalline change from the drug to the amorphous crystal. The *in-vivo* pharmacokinetic study was conducted using rabbits, and parameters of NAC-SLNs exhibited a significant rise in the  $C_{max}$ , AUC and oral absorption of the drug compared to the pure drug. Pharmacokinetic analysis revealed an 8.5-fold increase in bioavailability of the NAC-SLNs compared with NAC powder. In conclusion, NAC-SLNs have the potential to be an advantageous drug delivery technology for enhancing the oral performance of poorly soluble drugs.

**Keywords:** Entrapment efficiency, Hot-homogenization method, N- Acetylcysteine, Particle size, Solid lipid nanoparticles.

International Journal of Drug Delivery Technology (2022); DOI: 10.25258/ijddt.12.3.34

**How to cite this article:** Madupoju B, Raju RS, Desu PK, Rao GSNK, Alavala RR, Amara RD, Chakravarthi G. Development, Characterization and Optimization of N-acetylcysteine Loaded Solid Lipid Particles: *In-vitro* and *In-vivo* Study. International Journal of Drug Delivery Technology. 2022;12(3):1129-1135.

**Source of support:** Nil.

**Conflict of interest:** None

## INTRODUCTION

N-acetyl cysteine (NAC) has been used as a thiol-containing protective agent because its hepatoprotective characteristics have been demonstrated in various investigations.<sup>1-3</sup> N-Acetylcysteine (NAC) is a mucolytic, anti-inflammatory, and hepatoprotective chemical used as an antioxidant to protect cells and treat illnesses such as cancer, neuropsychiatric disorders, and cardiovascular disease.<sup>4</sup> Despite these benefits, NAC has a limited bioavailability (between 6 and 8%), limiting its therapeutic usefulness. It happens because it interacts with plasmatic proteins when it reaches the bloodstream and

generates disulfide bridges.<sup>6</sup> When taken intravenously, over 30% of NAC is lost in the urine, and high dosages might cause blood pressure to increase.<sup>5</sup> As a result, although researchers explore new ways to boost NAC bioavailability, developing carriers to transport and stabilize it inside the body is a significant challenge.<sup>6</sup>

Nanoparticles are dissolved and entrapped in active principles (drugs or physiologically active compounds) in colloidal particles having a diameter of 10 to 1000 nanometres.<sup>7</sup> A few examples include nanospheres, nanocapsules, dendrimers, solid-lipid nanoparticles, polymeric micelles,

\*Author for Correspondence: prasanna.desu@gmail.com

and liposomes. Advances in nanotechnology have made it feasible to create drug nanoparticles that can be employed in various ways.<sup>8</sup> Solid lipid nanoparticles (SLN) have sparked much interest in recent years because they offer several advantages over traditional colloidal drug delivery systems, including increased drug stability, increased protection against enzymatic metabolism, and the ability to deliver multiple drugs at once. Other benefits include controlled drug release, high drug loading capacity, biocompatibility, ease of large-scale production and sterilization, less variability in release mechanisms and kinetics, and the ability to deliver multiple drugs, simultaneously.<sup>9</sup>

Various lipid-based nano preparations improve poorly soluble compounds' solubility, absorption, and dissolution. Nano-sized SLNs with a unique shape and high drug loading capacity increase lipophilic drug absorption and receptor concentration. SLNs bypass apical transporter protein to increase therapeutic permeability.<sup>10</sup> They prevent medication acidification and improve vascular absorption. Particle size, %EE, and %CDR affect SLN physicochemical qualities.<sup>11</sup>

The purpose of this work was to develop SLNs of the mucolytic drug N-acetyl cysteine to improve their oral bioavailability and overcome difficulties such as low solubility.<sup>12</sup>

## MATERIALS AND METHODS

### Materials

NAC was obtained as a kind gift from Aravis labs Pvt. Ltd, Tamilnadu, India. The glyceryl monostearate, soya lecithin, span, and tweens were procured from Vijaya chemicals in Hyderabad. All other chemicals and reagents used in the present study were analytical grade.

### Preparation of NAC-SLNs

The hot homogenization technique developed NAC-SLN formulations. From the initial investigation, glyceryl monostearate (GM) and Soya lecithin (SL) were selected as solid lipids, and polysorbate 80 (PS-80), tween 40 and tween 80 were surfactants.<sup>13</sup> The detailed composition of prepared NAC-SLNs has been shown in Table 1. At a temperature of

10°C over the lipid's melting point, sufficient amounts of lipid, NAC, and lipophilic surfactants were weighed and combined in a water bath. Water and the hydrophilic surfactant were heated to the same temperature in a separate beaker and swirled constantly.<sup>14</sup> Drop by drop, the described lipid phase was added to the aqueous surfactant solution and agitated for a few hours at 3000 RPM.<sup>15</sup> After being sonicated for 60 minutes, the dispersion was retained. In the final step of the process, the prepared samples were allowed to drop to room temperature, after which the SLNs began to develop. In preparation for further examination, the sample was kept at a temperature of 4°C.<sup>16</sup>

## Characterization of NAC-SLNS

### Particle Size and PDI

The zeta sizer was used to investigate the PGL-SLNs in terms of their particle size and PDI (Malvern zeta sizer- 1000 HS, Malvern UK). The PGL-SLNs were diluted by a factor of 100 in a suitable solvent before being subjected to laser light scattering at a fixed angle of 90 degrees and a voltage of 50 millivolts.<sup>17</sup>

### Zeta Potential

The zeta potential of a particle indicates the overall charge of the particle as well as the stability of the formulation. The differential light scattering (DLS) technique was utilized to measure the zeta potential using the Zeta sizer Nano-ZS90, Malvern Instrument Ltd., UK. Nanoparticle samples were scattered using Milli-Q water. All measurements were made in triplicate at 25°C.<sup>17</sup>

### Determination of Entrapment Efficiency

The ultracentrifugation method was utilized to estimate the encapsulation effectiveness of the NCA-SLNs dispersion. After placing the NCA-SLNs in centrifugation tubes, they were placed in a cooling centrifuge (Sigma 3-1 KL IVD, Germany) and spun at 25,000 rpm for thirty minutes. After performing the necessary dilutions, the supernatant was separated, and its content of NCA was determined using a UV spectrophotometer.<sup>18</sup> This was done in triplicate. The %EE can be derived using the equation:

$$(EE) (\%) = (\text{Concentration of NCA in supernatant} / \text{Initial NCA concentration}) * 100$$

### Fourier Transform Infrared Spectroscopy (FT-IR) Study

The FT-IR spectrophotometer<sup>18</sup> was utilized to conduct the spectral study (PerkinElmer Spectrum One, Waltham, Massachusetts, USA). Using a resolution of 4 cm<sup>-1</sup>, the samples were analyzed using a scanning range from 4000 to 400 cm<sup>-1</sup>.

### Differential Scanning Calorimetry (DSC) Study

The compatibility research was conducted using Differential scanning calorimetry (DSC Q10 V9.0 Build 275). DSC analysis was performed on the natural drug and additional excipients to evaluate whether they were compatible with the medication.<sup>18</sup> The specific heat and transition enthalpies are determined using a differential scanning calorimeter. The area directly measures the heat of transition beneath the acquiring

**Table 1:** Formulation development of NAC-SLNs

F. no	NAC (mg)	GM (gms)	SL (mg)	PS-80	Tween 40 (mg)	Tween 80 (mg)
F1	50	0.25	50	100	50	100
F2	50	0.5	100	50	100	50
F3	50	0.75	50	100	50	100
F4	50	1	100	50	100	50
F5	50	1.25	50	100	50	100
F6	50	1.5	100	50	100	50
F7	50	1.75	50	100	50	100
F8	50	2	100	50	100	50
F9	50	2.25	50	100	50	100
F10	50	2.5	100	50	100	50
F11	50	2.75	50	100	50	100
F12	50	3	100	50	100	50

curve. A differential scanning calorimeter with a heating rate of 15°C/min and a temperature range of 0 to 1000°C was used to make the thermograms. The design gets hermetically sealed in an environment.

### XRD Study

The X-ray Diffractometer was used to analyze the crystalline characteristics of the samples (Bruker, Germany). To determine XRD patterns for NAC and the improved formulation, a Cu Ka radiation with a wavelength of 1.5406 was used in conjunction with a voltage of 40 kV and a current of 40 mA. The scans were performed at an angle range of 3–40° across a distance of 2 with a count time of 0.3 seconds and a step angle of 0.02°, respectively.<sup>18</sup>

### Scanning Electron Microscopy

The morphological appearance of the SLNs was directly observed by scanning electron microscopy, which provided a technique to keep the morphology of the SLNs directly. The particles were initially covered in gold to reduce the amount of heat generated by the high-power magnification, and they were then put through a scanning electron microscope machine (FEI Quanta2 hundred MK2 from the Netherlands) to capture images of the SLNs.<sup>19</sup>

### In-vitro Release Studies and Release Kinetics

An *in-vitro* drug release of NAC-SLNs formulation was developed using USP-II dissolving equipment (paddle apparatus) at 50 rpm. The test was conducted in 700 mL 0.1 N HCl for the first two hours, followed by 200 mL trisodium hydrogen phosphate to maintain a pH of 7.4. In thermostatically controlled water, the dissolving medium was kept at 37°C. To maintain the sink condition, 5 mL of the sample was withdrawn and replaced with an equivalent volume of a new medium at present time intervals. The materials were evaluated using the UV spectrophotometric method at a wavelength of 290 nm. The experiment was repeated three times to determine the percentage of medication release. The mechanism of drug release and its kinetics were assessed using mathematical models. The models best suited the data were chosen based on many models' correlation coefficient (R) values. The mathematical models employed were the Korsmeyer-Peppas model, the Higuchi model, the First-order release model, and the Zero-order release model.<sup>20</sup>

### In-vivo Pharmacokinetic Study

*In-vivo* pharmacokinetic study of NAC dispersion and NAC-SLN dispersion was performed on male wistar rats (7–8 weeks old, 220–280 g). An institutional animal ethics committee (IAEC), Nalanda College of Pharmacy, Nalgonda, approved the protocol to investigate the further study using rats (CPCSEA Reg No:318/Re/s/2001/CPCSEA, IAEC Approval No: NCOP/IAEC/00075). The rats were obtained from the animal house, where they were kept in normal environmental circumstances with a dark/light cycle that lasted for 12 hours. All rats were separated into two groups (each with six animals), with Group I receiving NCA dispersion and Group II

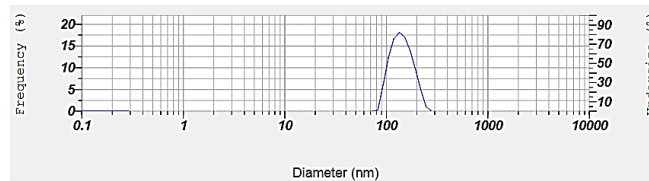


**Figure 1:** Particle size of all formulations of NAC-SLNs

receiving NCA-SLN dispersion.<sup>23</sup> The dispersion was given to rats at a dose of 0.5 mg/kg body weight via an oral feeding tube. Blood samples were taken from animals at 15, 30, 45, 60, 120, 180, 240, 480, 700, 1000, and 1400 minutes following administration using a retro-orbital bleeding technique. The blood samples were centrifuged for 10 minutes at 3000 rpm, and the plasma samples were kept at 20°C until analysis.<sup>24</sup> Before HPLC, the samples were passed through 0.22 µm membrane filters. The liquid chromatography process of the substance in rat plasma was used to purify the sample before examination further. The plasma drug concentration versus time plot was developed, and different pharmacokinetic drug parameters were used to evaluate the drug absorption and distribution rate in the body.<sup>21</sup>

## RESULTS AND DISCUSSION

### Particle Size, Polydispersity Index and Zeta Potential

The particle size of NAC-SLNs was between  $79 \pm 11.27$  to and  $159.10 \pm 15.36$  with PDI of 0.112 to 0.168. The results are shown in Table 2. The results revealed that all SLNs were found to be distributed within the nano size. The particle size of nanoparticles was reduced due to an increase in the concentration of both lipid and surfactant, which contributed to the reduction. From Table 2, the zeta potential was discovered in the range of -51.32 to -39.13 mV, and the NAC-SLNP's potential was realized. According to the studies of the effects of Zeta potential, every formulation was found to be Table. The size distribution of solid lipid nanoparticles for our inspection is in Figure 1.

**Table 2:** Evaluation studies of particle size nanoparticles

F. no	Particle size (nm)	PDI	ZP(mV)	%EE
F1	96.23 ± 9.98	0.118	-42.03	71.25 ± 1.25
F2	100.36 ± 10.2	0.122	-39.13	63.59 ± 1.89
F3	99.23 ± 11.21	0.121	-48.36	82.35 ± 1.42
F4	125.12 ± 11.8	0.138	-49.47	75.25 ± 1.63
F5	149.56 ± 10.8	0.146	-51.32	73.18 ± 1.50
F6	132.16 ± 14.89	0.14	-39.32	78.95 ± 2.01
F7	98.69 ± 9.67	0.121	-40.12	68.93 ± 0.99
F8	135.40 ± 8.93	0.144	-42.20	62.56 ± 1.25
F9	120 ± 10.78	0.127	-43.32	80.69 ± 1.32
F10	159.10 ± 15.36	0.168	-50.33	86.32 ± 1.24
F11	149 ± 13.85	0.148	-49.28	84.36 ± 1.24
F12	79 ± 11.27	0.112	-42.16	80.21 ± 1.86

### Entrapment Efficiency

All 12 formulations were tested for drug entrapment efficiency; the results are shown in Table 2. The entrapment efficiency for NAC-SLNPs ranged from  $62.56 \pm 1.25\%$  to  $86.32 \pm 1.24$ . From the results, it was revealed that the concentration of lipid increased, and the entrapment efficiency increased.

### Fourier Transform Infrared Spectroscopy (FT-IR) Study

Figures 2 and 3 demonstrate the FT-IR spectra obtained for the pure drug and its physical combination, respectively. Not a single spectrum lacks any functional peaks, meaning that all of these peaks were present in the drug itself and the physical mixture. As a result, it was discovered that the formulation's medication and lipid do not engage in any meaningful physicochemical interaction.

### X-ray Diffraction Analysis (XRD) Study

Figures 4 and 5 present the pure drug's XRD spectra and the physical mixture, respectively. The crystalline nature of the substance was revealed by the presence of distinctive peaks in the diffraction spectrum of the pure drug. However, the strength of each of the primary peaks of NAC was much lower, even though they were all present in the same location in the physical combination. Raloxifene did not have any crystalline peaks when it was formulated as SLN, indicating that the medication did not exist in crystalline form. In the SLN formulation, there was also a reduction in the intensity of the pure lipid peaks. This reduced intensity provides further evidence that the lipid in SLN formulation has a reduced crystallinity.

### DSC Study

A DSC study was carried out to determine any interactions between the components. The DSC thermograms of the medication in its purest form are displayed in Figure 6. Due to the crystalline structure of NAC, an endothermic peak could be seen at a relatively high temperature of  $157.1^\circ\text{C}$ . Figure 7 presents an image of the DSC for the physical mixture. NAC has an exothermic abrupt peak at a temperature of  $207^\circ\text{C}$  due to the drug's breakdown. In addition, the endothermic peak seen at a temperature of  $290^\circ\text{C}$  can be attributed to the melting of the product of the study of NAC.

### SEM Study

The NAC-SLNPs were found to be spherical using scanning electron microscopy. The nanoparticles' surfaces were smooth. Particles with a diameter of less than 200 nm were found in most cases. The nanoparticles' surfaces were smooth, as shown in Figure 8.

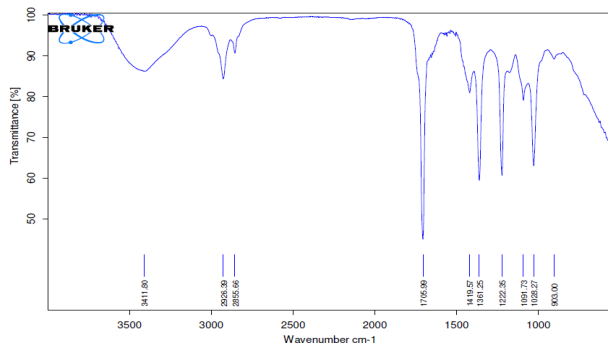


Figure 2: FT-IR spectra of NAC

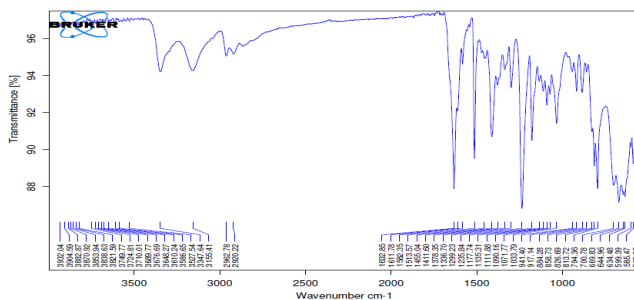


Figure 3: FT-IR spectra of physical mixture of drug and excipients

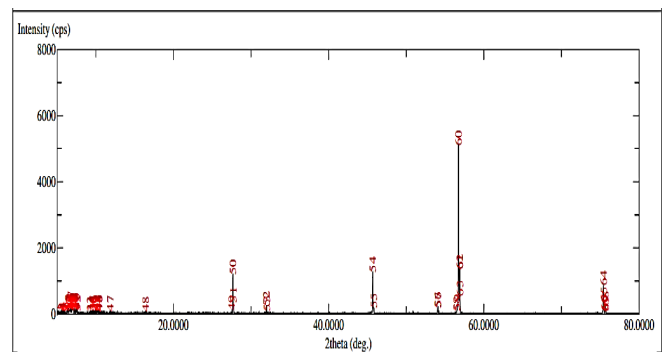


Figure 4: XRD spectra of NAC

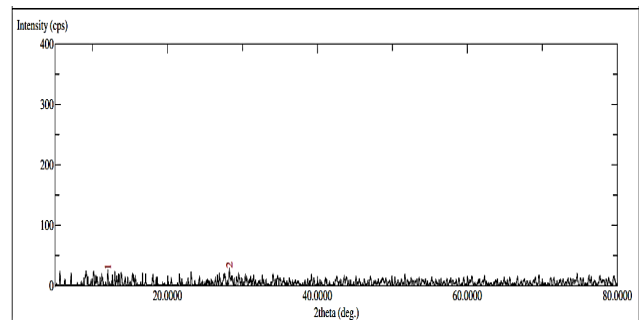


Figure 5: XRD spectra of Optimized formulation

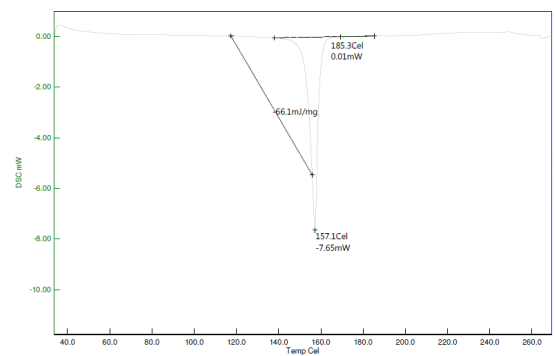


Figure 6: DSC spectra of NAC

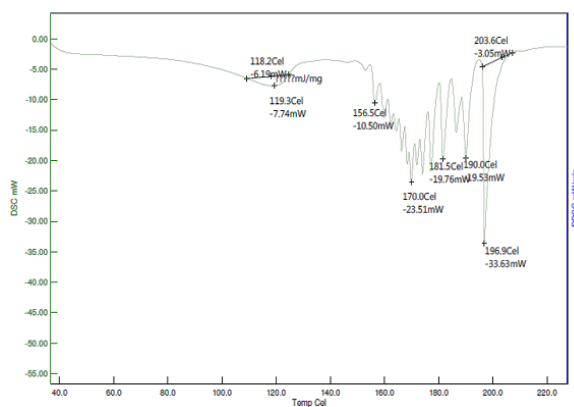


Figure 7: DSC Analysis of optimized formulation

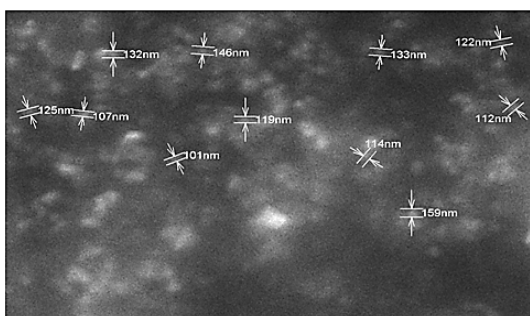


Figure 8: SEM Analysis of nanoparticles

### *In-vitro* Drug Release Studies

The drug release from the polysorbate 80 prepared SLNs was faster and more sustained than from the Tween 40 and 80-prepared SLNs. This might be because smaller particles have more surface area and shorter diffusion lengths, resulting in faster disintegration and drug release. Dissolution equipment was used to conduct drug release tests on all N-acetylcysteine

SLN formulations over 8 hours. The findings of the drug release trials, as shown in Figure 9 and Table 3, revealed that the 10th formulation had the highest drug release rate of 95.25% within 8 hours. To determine the release behaviour of ACN from the prepared SLNs, the release kinetics for all of the prepared ACN-SLNs were studied. The release data were evaluated using the Higuchi kinetic model and zero-order, first-order, and Korsmeyer–Peppas kinetic models. The Higuchi kinetic model with the greatest ( $r$ ) value of 0.995 fits the release data from SLNs, but the zero-order kinetic model provides the release data from free ACN nanoparticles.

### *In-vivo* Pharmacokinetic Study

To generate plasma calibration points, 100  $\mu$ L of biological matrices were injected with 10  $\mu$ L of a different NAC standard solution. The plasma calibration curve had a range of 0.25 to 100 g/mL and included individual calibration points at 100, 50, 25, 10, 5, 2.5, 1, 0.5, and 0.25 g/mL. Sample preparation After diluting the plasma to a total volume of one hundred litres with distilled water, 50 L of a DTT solution containing 0.5% was added. The mixture was vortexed for ten seconds. After each tube had been heated for 30 minutes in a water bath at 37°C, 100 microliters of 0.5 M NaHCO<sub>3</sub> and 12.5 microliters of 5% DNFB (in methanol) were added to it, and then the tubes were vortexed for 30 seconds. After that, the tubes were covered in aluminous foils and put back into the incubator for another half an hour at 60°C. After bringing the samples to room temperature, 700 microliters of diethyl ether were added to each sample. Then the samples were vortexed for thirty seconds before being centrifuged at 5000 revolutions per minute for five minutes. Following the removal of the supernatants, 100  $\mu$ L of 6 M HCl and 700 L of diethyl ether were added to the mixture. Before centrifuging all of the samples at 5000 rpm for five minutes, each sample was given a 60-seconds whirl in a vortex. After being separated into clean tubes, the supernatants

Table 3: *In-vitro* drug release studies of NAC-SLNs formulations

Time (hours)	F1	F2	F3	F4	F5	F6	F7	F8	F9	F10	F11	F12
0	0	0	0	0	0	0	0	0	0	0	0	0
1	10.23 ± 0.23	11.25 ± 0.52	14.22 ± 0.68	15.32 ± 0.75	12.35 ± 0.80	15.78 ± 0.54	13.69 ± 0.52	14.18 ± 1.20	12.97 ± 0.32	16.12 ± 0.25	11.25 ± 0.29	15.34 ± 0.52
2	23.31 ± 0.52	27.10 ± 0.48	21.18 ± 0.32	22.65 ± 0.82	20.19 ± 0.32	24.21 ± 0.63	21.32 ± 0.46	25.63 ± 0.96	22.32 ± 0.25	25.18 ± 0.46	20.38 ± 0.37	23.41 ± 0.64
3	35.40 ± 0.48	32.21 ± 0.27	38.30 ± 0.65	37.21 ± 1.34	36.59 ± 0.56	32.28 ± 0.93	34.45 ± 0.52	33.51 ± 1.05	35.21 ± 0.54	40.17 ± 0.37	39.32 ± 0.79	38.93 ± 0.73
4	41.58 ± 0.29	45.17 ± 0.45	44.35 ± 0.75	45.31 ± 0.93	42.35 ± 0.70	41.50 ± 0.13	40.32 ± 0.49	43.29 ± 0.63	42.67 ± 0.63	51.28 ± 0.42	46.53 ± 0.24	43.82 ± 0.25
5	53.32 ± 0.31	53.24 ± 0.12	59.24 ± 0.55	61.52 ± 1.20	60.31 ± 0.53	52.25 ± 0.34	52.86 ± 0.63	54.52 ± 0.51	55.36 ± 0.87	63.74 ± 0.46	60.24 ± 0.51	58.34 ± 0.43
6	65.17 ± 1.20	65.42 ± 0.59	71.60 ± 0.54	74.32 ± 0.98	68.93 ± 0.46	66.54 ± 0.61	63.42 ± 0.37	68.28 ± 0.84	70.21 ± 0.46	78.25 ± 0.53	75.98 ± 0.42	73.15 ± 0.60
7	73.89 ± 0.32	73.10 ± 0.37	83.20 ± 0.61	86.21 ± 0.51	79.32 ± 0.51	73.28 ± 0.67	76.37 ± 0.34	78.25 ± 0.61	81.25 ± 0.51	87.32 ± 0.57	88.31 ± 0.34	83.54 ± 1.23
8	86.85 ± 0.54	81.56 ± 0.38	92.56 ± 0.53	93.28 ± 0.55	86.27 ± 0.53	91.75 ± 0.50	90.84 ± 0.28	88.98 ± 0.53	93.24 ± 0.32	95.25 ± 0.46	90.86 ± 0.25	92.35 ± 0.36

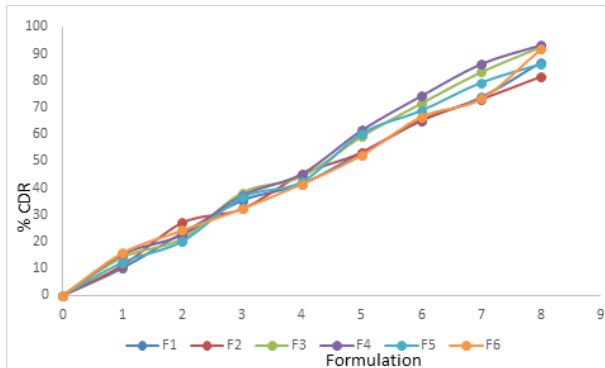


Figure 9: *In-vitro* drug release studies of (F1-F6) formulations

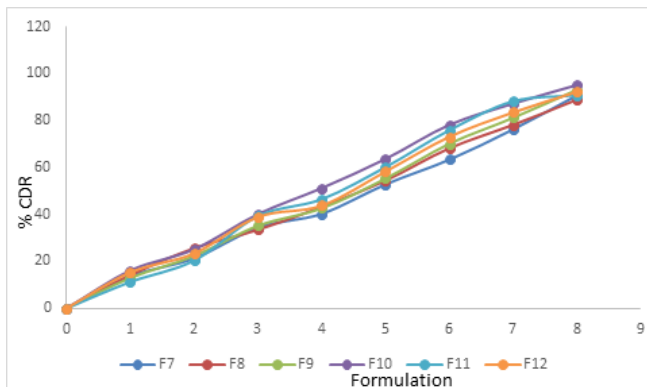


Figure 10: *In-vitro* drug release studies of (F7-F12) formulations

were evaporated at a low temperature (40°C) until they were dry. After reconstituting in 100 L of 50 mM trisodium citrate and 1-mM disodium EDTA, the residue was loaded onto the HPLC column (pH 7.0) (Figure 10).

#### Pharmacokinetics of N-Acetyl cysteine (NAC)

It was found that. The mean peak plasma concentration ( $C_{max}$ ) for N-Acetyl cysteine after administration of the NAC-dispersion and NAC-SLN-dispersion were found to be  $6.01 \pm 0.01$  and  $5.99 \pm 0.02$  ng/mL, respectively. The time to peak concentration ( $t_{max}$ ) for N-Acetyl cysteine after administration of NAC-dispersion and NAC-SLN-dispersion were 441 and

Table 4: Pharmacokinetic parameters of NAC-dispersion and NAC-SLN-dispersion

Parameter	NAC-dispersion	NAC-SLN-dispersion
$t_{1/2}$ (min)	$33 \pm 1.02$	$34 \pm 2.06$
$C_{max}$ (ng/mL)	$6.01 \pm 0.01$	$5.99 \pm 0.02$
$T_{max}$ (min)	441	421
$K_e$ ( $\text{min}^{-1}$ )	0.021	0.020
$K_a$ ( $\text{min}^{-1}$ )	0.21	0.37
CL( $\text{mL}/\text{min}/\text{kg}$ )	$47.95 \pm 8.61$	$51.23 \pm 6.14$
$V_{ss}$ ( $\text{mL}/\text{kg}$ )	$602.4 \pm 21.3$	$711 \pm 19.07$
$AUC_{0-\infty}$ (ng/mL. min)	$3465.32 \pm 11.31$	$3890.87 \pm 10.21$
$AUMC_{0-\infty}$ (ng/mL. $\text{min}^2$ )	$14951 \pm 51.24$	$18821 \pm 41.33$
MRT	$4.31 \pm 0.14$	$4.83 \pm 0.11$

Mean  $\pm$  SD, n=6

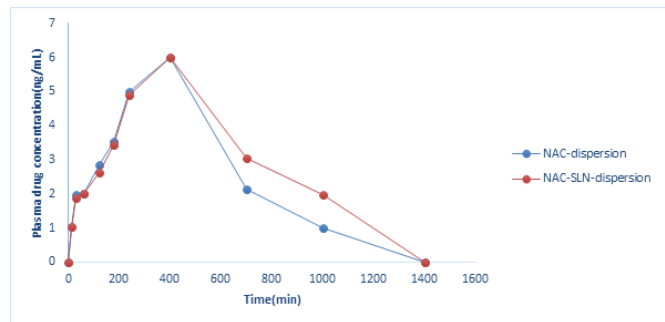


Figure 11: Pharmacokinetic parameters of NAC-dispersion and NAC-SLN-dispersion

421 minutes, respectively. After administration of the NAC-dispersion and NAC-SLN-dispersion, the area under the plasma concentration-time curve ( $AUC_{0-t}$ ) for N-Acetyl cysteine was determined to be  $3465.32 \pm 11.31$  and  $3890.87 \pm 10.21$  ng/mL, respectively. The higher AUC value of NAC-SLN-dispersion refers to higher bioavailability than NAC-SLN-dispersion. The higher values of absorption rate constant ( $K_a$ ), steady-state volume of distribution ( $V_{ss}$ ), drug clearance (CL), and mean residence time (MRT) indicates the targeting nature of NAC-SLN dispersion when compared to NAC-dispersion (Figure 11 and Table 4).

#### CONCLUSION

The potential application of SLNs for the prolonged release of n acetylcysteine, which is utilized to target liver & lung infections, was proven in this work. According to the results of the FT-IR investigation, there is no interaction between the medicine and the excipients. The thermal homogenization method yielded N-acetylcysteine-SLNs with a high EE, particle size distribution, and zeta potential. The N acetylcysteine solid lipid nanoparticles showed a sustained-release impact in an *in-vitro* release experiment. When compared to NAC-SLN-dispersion, NAC-SLN-dispersion had a greater AUC value, indicating better bioavailability and targeting activity in the present *in-vivo* pharmacokinetic study.

#### ACKNOWLEDGEMENTS

The authors would like to acknowledge the Nalanda college of pharmacy for providing the facilities to carry out the research work.

#### CONFLICT OF INTEREST

There is no conflict of interest.

#### REFERENCES

- Flanagan RJ, Meredith TJ. Use of N-acetylcysteine in clinical toxicology. The American journal of medicine. 1991 Sep 30;91(3):S131-9. DOI: 10.1016/0002-9343(91)90296-a.
- Shah KR, Beuhler MC. Single bag high dose intravenous N-acetylcysteine associated with decreased hepatotoxicity compared to triple bag intravenous N-acetylcysteine in high-risk acetaminophen ingestions. Clinical Toxicology. 2022 Apr 3;60(4):493-8. <https://doi.org/10.1080/15563650.2021.1979231>.

3. Minhaj FS, Leonard JB, Seung H, Anderson BD, Klein-Schwartz W, King JD. *In-vitro* analysis of n-acetylcysteine (NAC) interference with the international normalized ratio (INR). *Clinical Toxicology*. 2022 Apr 3;60(4):489-92. <https://doi.org/10.1080/15563650.2021.1979232>.
4. Fatima M, Kamran M, Zehra S, Jamil N, Zaidi IH. Histopathological effects with marwar teak (*tecomella undulata*) bark extract and N-acetylcysteine on acetaminophen induced hepatotoxicity in albino rats. *The Professional Medical Journal*. 2022 Feb 28;29(03):345-50. <https://doi.org/10.1002/2211-5463.13449>.
5. Motafeghi F, Mortazavi P, Salman Mahiny AH, Abtahi MM, Shokrzadeh M. The role of ginger's extract and N-acetylcysteine against docetaxel-induced oxidative stress and genetic disorder. *Drug and Chemical Toxicology*. 2022 May 13:1-8. <https://doi.org/10.1080/01480545.2022.2075377>.
6. Singh J, Phogat A, Kumar V, Malik V. N-acetylcysteine ameliorates monocrotophos exposure-induced mitochondrial dysfunctions in rat liver. *Toxicology Mechanisms and Methods*. 2022 Apr 20:1-9. <https://doi.org/10.1080/15376516.2022.2064258>.
7. Müller RH, Mäder K, Gohla S. Solid lipid nanoparticles (SLN) for controlled drug delivery—a review of the state of the art. *European journal of pharmaceuticals and biopharmaceutics*. 2000 Jul 3;50(1):161-77. [https://doi.org/10.1016/S0939-6411\(00\)00087-4](https://doi.org/10.1016/S0939-6411(00)00087-4).
8. Paliwal R, Paliwal SR, Kenwat R, Kurmi BD, Sahu MK. Solid lipid nanoparticles: A review on recent perspectives and patents. *Expert opinion on therapeutic patents*. 2020 Mar 3;30(3):179-94. <https://doi.org/10.1080/13543776.2020.1720649>
9. Weber S, Zimmer A, Pardeike J. Solid lipid nanoparticles (SLN) and nanostructured lipid carriers (NLC) for pulmonary application: a review of the state of the art. *European Journal of Pharmaceutics and Biopharmaceutics*. 2014 Jan 1;86(1):7-22. <https://doi.org/10.1016/j.ejpb.2013.08.013>
10. Gordillo-Galeano A, Mora-Huertas CE. Solid lipid nanoparticles and nanostructured lipid carriers: A review emphasizing on particle structure and drug release. *European Journal of Pharmaceutics and Biopharmaceutics*. 2018 Dec 1;133:285-308. <https://doi.org/10.3329/icpj.v1i11.12065>
11. Garcês A, Amaral MH, Lobo JS, Silva AC. Formulations based on solid lipid nanoparticles (SLN) and nanostructured lipid carriers (NLC) for cutaneous use: A review. *European Journal of Pharmaceutical Sciences*. 2018 Jan 15;112:159-67. <https://doi.org/10.1016/j.ejps.2017.11.023>
12. Rishitha N, Muthuraman A. Therapeutic evaluation of solid lipid nanoparticle of quercetin in pentylenetetrazole induced cognitive impairment of zebrafish. *Life sciences*. 2018 Apr 15;199:80-7. <https://doi.org/10.1016/j.lfs.2018.03.010>
13. Dudhipala N. A comprehensive review on solid lipid nanoparticles as delivery vehicle for enhanced pharmacokinetic and pharmacodynamic activity of poorly soluble drugs. *International Journal of Pharmaceutical Sciences and Nanotechnology*. 2019 Mar 31;12(2):4421-40. <https://doi.org/10.37285/ijpsn.2019.12.2.1>
14. Khames A, Khaleel MA, El-Badawy MF, El-Nezhawy AO. Natamycin solid lipid nanoparticles—sustained ocular delivery system of higher corneal penetration against deep fungal keratitis: preparation and optimization. *International Journal of Nanomedicine*. 2019;14:2515. <https://doi.org/10.2147%2FIJN.S190502>.
15. Duong VA, Nguyen TT, Maeng HJ. Preparation of solid lipid nanoparticles and nanostructured lipid carriers for drug delivery and the effects of preparation parameters of solvent injection method. *Molecules*. 2020 Oct 18;25(20):4781. <https://doi.org/10.3390/molecules25204781>
16. El-Housiny S, Shams Eldeen MA, El-Attar YA, Salem HA, Attia D, Bendas ER, El-Nabarawi MA. Fluconazole-loaded solid lipid nanoparticles topical gel for treatment of pityriasis versicolor: formulation and clinical study. *Drug delivery*. 2018 Jan 1;25(1):78-90. <https://doi.org/10.1080/10717544.2017.1413444>.
17. Pandian SR, Pavadai P, Vellaisamy S, Ravishankar V, Palanisamy P, Sundar LM, Chandramohan V, Sankaranarayanan M, Panneerselvam T, Kunjiappan S. Formulation and evaluation of rutin-loaded solid lipid nanoparticles for the treatment of brain tumor. *Naunyn-Schmiedeberg's Archives of Pharmacology*. 2021 Apr;394(4):735-49. <https://doi.org/10.1007/s00210-020-02015-9>.
18. Asif AH, Desu PK, Alavala RR, Rao GS, Sreeharsha N, Meravanige G. Development, Statistical Optimization and Characterization of Fluvastatin Loaded Solid Lipid Nanoparticles: A 32 Factorial Design Approach. *Pharmaceutics*. 2022 Mar 8;14(3):584. <https://doi.org/10.3390/pharmaceutics14030584>
19. Araujo VH, Delello Di Filippo L, Duarte JL, Sposito L, Camargo BA, da Silva PB, Chorilli M. Exploiting solid lipid nanoparticles and nanostructured lipid carriers for drug delivery against cutaneous fungal infections. *Critical reviews in microbiology*. 2021 Jan 2;47(1):79-90. <https://doi.org/10.1080/1040841X.2020.1843399>.
20. Rampaka R, Ommi K, Chella N. Role of solid lipid nanoparticles as drug delivery vehicles on the pharmacokinetic variability of Erlotinib HCl. *Journal of Drug Delivery Science and Technology*. 2021 Dec 1;66:102886. <https://doi.org/10.1016/j.jddst.2021.102886>.
21. Paliwal HP, Prajapati BG, Khunt D, Shirisha C, Patel JK, Pathak YV. Pharmacokinetic and Tissue Distribution Study of Solid Lipid Nanoparticles. In *Pharmacokinetics and Pharmacodynamics of Nanoparticulate Drug Delivery Systems 2022* (pp. 245-260). Springer, Cham. [https://doi.org/10.1007/978-3-030-83395-4\\_13](https://doi.org/10.1007/978-3-030-83395-4_13).